

First go at a field map for Magnet NDB21 in MTest

November 2009

Abstract

This note describes results of a trial construction of a field map for the downstream NDB magnet (NDB21) in the tertiary beamline in MTest. The preliminary map is simplified and incomplete in several ways, but does cover the entire gap of the magnet. That map, in turn, is inserted into a Root-based 3D histogram which has a built-in interpolation function, and also Runge-Kutta stepper software routine, and is used to examine particle trajectories through this field.

This exercise is a step toward a refined field map for the magnet pair and demonstrates some operational tools for the reconstruction of particle momenta and an exploration of the accuracy needed to achieve the MINERvA precision goals. It is also a learning exercise for MINERvA personnel who had no prior, specific experience with precision field mapping or momentum reconstruction.

1 Introduction

Two small dipole magnets of the NDB type are installed in the MTest experimental area for use in a low-momentum tertiary beamline. Using the magnets, the measured magnetic field, and a set of wire chambers, the momenta of particles traversing the beamline can be measured.

For three days in mid-October 2009, Doug Jensen and Jerry Zimmerman used a precision three-axis Hall probe, a monitor probe, a LabView based DAQ program, plus a stand and pegboard put together by Todd Nebel, and took measurements of the field of the upstream NDB22 magnet. On Thursday 29 October, they provided the equipment and software to the MINERvA experimenters, and Lee Patrick, David Martinez, and Rik Gran spend the day taking measurements of the field of the downstream NDB21 magnet. The field in this note is based on that last day of measurements and for that single magnet.

The power supply was set to ramp to 100A and hold that current for approximately 5 seconds, and using a pulse generator, it repeated this ramp with the roughly one-minute cycle time typical of beam operations at MTest. The LabView software was set to record the data more extreme than some nominal threshold for the principle component of the field. The data includes a time stamp. In addition, the reading from a monitor probe affixed to the magnet, the location of the precision probe on the peg board, and the time were recorded in David's lab book for most data points, to be attached later to the measured precision data.

In general, the minute between ramps was enough time for moving the magnet probe to the new position and double checking it. At this speed, we were able to take three complete zips, two with one spacer block on the H and B columns (points along the beam axis through the magnet), plus one with three spacer blocks along the H column. We also took repeated measurements at the same position (H7) on several occasions, and took transverse scans on rows 7, 8, 17, 32, and 33; the last two are in the gap between magnets.

The field measurements used for the map were extracted from the raw data by David Martinez and Rik Gran. We used a spreadsheet to look at the data and to take an average of 15 or 16 data points through the flat-top. For some measurements, there were fewer data points, so our average included fewer. For a few measurements, there was an apparent DAQ failure, and several seconds of data were missing where a flattop should have been. The ADC offset is subtracted based on the measurement of a zero field taken at the edge of the pegboard far from the magnet, and the result is converted to Gauss using the factor given by Doug: divide the raw value by 209. We have taken the error on the resulting field measurement to be the RMS/\sqrt{N} , and a typical random error for the principal component extracted this way is about one Gauss, though other systematic and random errors are larger.

2 Constructing the field map

By construction, this map has its origin centered in the middle of the magnet, and takes the z axis to be the beam axis through that center. The right-handed coordinate system then has x axis horizontal to the right, and the y component vertical with the $+y$ going downward toward the floor. In this coordinate system, the measurements from the Hall probe with a large -3300 Gauss principal component correspond to a $B_y = +3300$ Gauss, a downward pointing field that will bend positive particles to the left $= -x$ axis.

In constructing the field map for one magnet, I took the field measurements coming out of the magnet, downstream from the beam's view. Putting the measured fields in a spreadsheet, I formed the field for a 2-D quadrant, shown in the table below. The points in between measurements were formed assuming the trend from the nearest transverse and longitudinal scans hold approximately true, plus I continued the exponential fall-off of the field beyond the measured values down to a few Gauss. Then I assumed symmetry and copied this quadrant over to fill the other three quadrants. In order to proceed with some additional tests, I have temporarily taken this 2D field to have no Y dependence, which is obviously not true.

It is clear that this exercise has produced a field whose accuracy is not perfect, and we will want to refine it. It is also clear that even this first pass was a useful experience. Specific shortcomings of this field model:

- This field includes only the B_y component.
- This field has only xz dependence, in effect it is $B_y(x,z)$.
- It is the field for a single magnet, not both together.
- It does not include the field return in the magnet steel.
- We made only a casual attempt to confirm the pegboard coordinate system is centered.
- No corrections for thermal drift of magnet components, or probe.
- A future mapping campaign can include intermediate points.
- In the end, we need the field for both magnets as installed.
- Metal pieces have since been installed to cool the coils, which may slightly modify the field.

By (Gauss)		A	B	C	D	E	F	G/H
	position	16.51cm	13.97 cm	11.43 cm	8.89 cm	6.35 cm	3.81 cm	1.27 cm
-9	68.58 cm	0.00	0.00	0.00	0.00	0.00	0.00	0.00
-8	66.04 cm	2.94	3.07	3.19	3.32	3.45	3.58	3.71
-7	63.50 cm	4.39	4.58	4.77	4.96	5.15	5.34	5.53
-6	60.96 cm	6.55	6.84	7.12	7.41	7.69	7.98	8.27
-5	58.42 cm	9.78	10.21	10.64	11.06	11.49	11.92	12.34
-4	55.88 cm	14.61	15.25	15.88	16.52	17.16	17.80	18.44
-3	53.34 cm	21.82	22.77	23.72	24.67	25.63	26.58	27.53
-2	50.80 cm	32.58	34.00	35.43	36.85	38.27	39.70	41.12
-1	48.26 cm	48.66	50.78	52.91	55.03	57.16	59.28	61.41
0	45.72 cm	72.72	75.89	79.07	82.24	85.42	88.59	91.77
1	43.18 cm	105.16	109.63	114.11	118.59	123.07	127.54	132.02
2	40.64 cm	153.50	160.29	167.09	173.88	180.68	187.47	194.26
3	38.10 cm	230.33	240.02	249.70	259.39	269.07	278.76	288.44
4	35.56 cm	352.33	363.33	425.17	432.10	435.68	436.00	436.00
5	33.02 cm	537.78	565.85	648.95	659.54	665.01	665.49	665.49
6	30.48 cm	822.71	883.92	992.79	1008.98	1017.35	1018.08	1018.08
7	27.94 cm	1227.86	1362.77	1481.70	1505.87	1518.35	1519.45	1519.45
8	25.40 cm	1727.65	1978.72	2084.82	2118.82	2136.39	2146.83	2145.06
9	22.86 cm	2195.62	2585.66	2649.54	2692.75	2715.08	2717.04	2717.04
10	20.32 cm	2498.43	2985.36	3014.96	3064.13	3089.54	3091.77	3091.77
11	17.78 cm	2643.70	3167.29	3190.26	3242.29	3269.17	3271.54	3271.54
12	15.24 cm	3145.19	3233.26	3321.33	3334.53	3337.35	3333.98	3337.35
13	12.70 cm	3167.61	3256.62	3345.63	3358.94	3361.77	3358.38	3361.77
14	10.16 cm	3173.99	3263.88	3353.78	3367.11	3369.96	3366.56	3369.96
15	7.62 cm	3176.65	3267.41	3358.16	3371.52	3374.36	3370.96	3374.36
16	5.08 cm	3017.87	3268.83	3361.16	3374.52	3374.16	3373.97	3377.37
17	2.54 cm	3019.12	3269.84	3362.56	3375.93	3375.56	3375.37	3378.78
18	0.00 cm	3020.04	3267.97	3363.57	3376.95	3376.58	3376.39	3379.80

Table 1: Values used in the field map. Measured points (with one vertical spacer on the probe) are from the H column and B column zip, and transverse scans in row 8 and row 17, with the exception of negative rows for column H which were calculated assuming a continued exponential fall-off, and the value for H4 where the readout failed. The one inch intervals on the pegboard are translated to cm, row 18 is assumed to be the approximate longitude center of the magnet, while the transverse center is assumed to be halfway between G and H. The full map based on the quadrant above, is reflected around the z and x symmetry axes and extended uniformly on 2.54 cm spaced points in the y direction, and zeros for the B_y or B_z components and then dumped into a text file with the space delimited format: x y z Bx By Bz.

3 Using the field map

The first pass field map can already be used to study the trajectories of particles passing through a single magnet, in the xz plane, as long as they do not stray too close to the edge. Indeed, the goal of this exercise is to quickly complete the chain from measurement to map to trajectories to momentum reconstruction.

To do this we are using some software written by and/or copied and assembled by Lee Patrick, and modified by Rik Gran to accommodate a field map constructed as above. This software includes a 4th order Runge-Kutta stepping algorithm, with no accommodation for scattering or energy loss. It also uses the Root 3D histogram class, which has a built-in trilinear interpolation method, which is available in the latest version of Root 5.24, and possibly other recent versions. The last piece of the puzzle, using this software to determine a reconstructed trajectory and best value for the momentum is still in development.

Using these tools, I have sent a 1.0 GeV positive charged particle with an initial trajectory along the z axis at $x=y=0.0$ cm. It exits the field region with a $P_t = 57.31$ MeV/c and crosses a plane at $z = 500$ at $x = -28.7$ cm (and $y = 0.0$ because there are no B_x or B_z components in the field map). The integrated $B_y dl$ for this trajectory is 191.265 kGauss cm, and is consistent with the $P_t = 0.29979 B_y dl = 57.34$ MeV (with B_y in kGauss and dl in cm).

Because the field is not uniform, 1.0 GeV particles with incident trajectories will see different field integrals and end up with different transverse momenta. The following figure is a scan across the X axis. The left three points are unphysical because the fieldmap artificially cuts off at the left edge, and the particle trajectory crosses this edge before leaving the field region in z . For trajectories with $x = +10.5$ and -9.0 cm, the transverse momentum is systematically about 1% different than at dead center. The physical edge of the aperture should be at 15.875 cm.

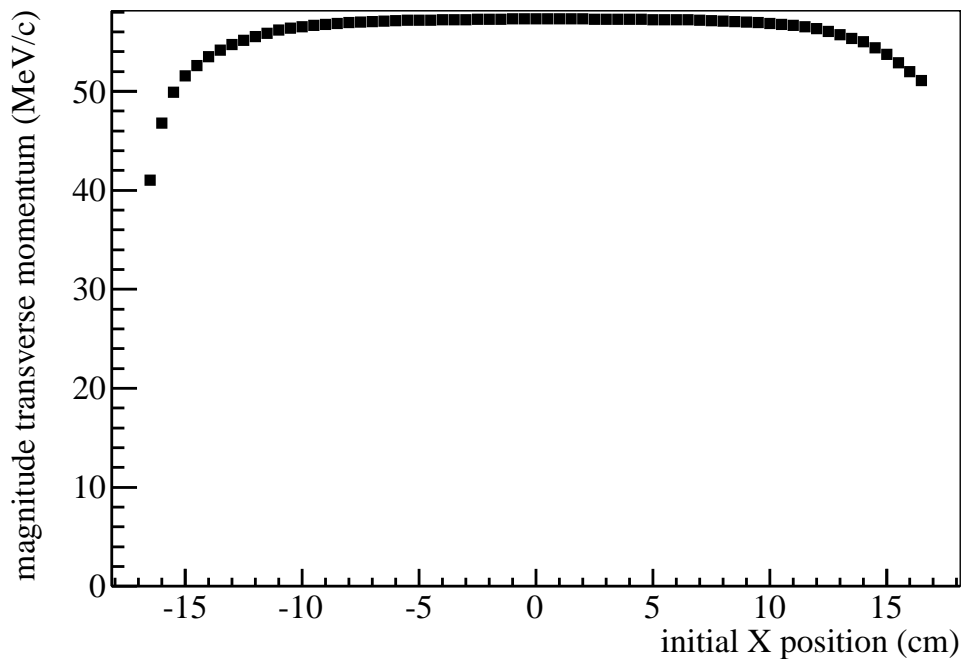


Figure 1: Resulting transverse momentum for input trajectories at different values of X. The left most three points are unphysical, the 1.0 GeV particle leaves the field region into the steel or at the edge where the field map artificially cuts off to zero.